

see page 6

Nectin-1 Expression by Squamous Cell Carcinoma is a Predictor of Herpes Oncolytic Sensitivity

Zhenkun Yu^{1,2}, Prasad S Adusumilli³, David P Eisenberg³, Elizabeth Darr¹, Ronald A Ghossein⁴, Sen Li¹, Shiquan Liu¹, Bhuvanesh Singh¹, Jatin P Shah¹, Yuman Fong³ and Richard J Wong¹

¹Head and Neck Service, Department of Surgery, Memorial Sloan-Kettering Cancer Center, New York, New York, USA; ²Department of Otolaryngology, Beijing Tongren Hospital, Capital University of Medical Sciences, Beijing, China; ³Hepatobiliary Service, Department of Surgery, Memorial Sloan-Kettering Cancer Center, New York, New York, USA; ⁴Department of Pathology, Memorial Sloan-Kettering Cancer Center, New York, New York, USA

Oncolytic viruses based on herpes simplex virus type 1 (HSV-1) are able to infect and lyse a variety of malignant cell lines. However, there is variability in the degree of tumor susceptibility, and the cancer cell determinants of HSV sensitivity are poorly defined. Nectin-1 is a cell surface adhesion molecule that functions as a cellular receptor to HSV envelope glycoprotein D (gD). We assessed tumor nectin-1 expression as a predictor of oncolytic HSV sensitivity. A panel of human squamous carcinoma cell lines was evaluated for viral entry, replication, and cytotoxicity to an attenuated, replication-competent, oncolytic HSV (NV1023). Potential tumor determinants of HSV sensitivity were assessed, including nectin-1, herpes viral entry mediator, total gD receptor expression, S-phase fraction, and doubling time. Significant correlations between nectin-1 expression measured by quantitative fluorescence-activated cell sorting and viral sensitivity measures were identified using Pearson's coefficients. Cancer cell nectin-1 receptor blockade and nectin-1 transfection led to inhibition and enhancement of NV1023 viral entry, respectively. Cell lines with varying nectin-1 expression showed corresponding sensitivity to NV1023 therapy *in vivo*. Immunohistochemistry for nectin-1 was inversely related to E-cadherin staining, suggesting increased herpes sensitivity of E-cadherin-deficient tumors. These results suggest that nectin-1 may be used as a marker to predict the sensitivity of a tumor to herpes oncolytic therapy.

Received 13 April 2006; accepted 6 August 2006.
doi:10.1038/sj.mt.6300009

INTRODUCTION

Attenuated, replication-competent viruses based on herpes simplex virus type 1 (HSV-1) have been engineered with significantly reduced neurotoxic effects as compared to wild-type

HSV-1.¹⁻⁴ These attenuated vectors possess an ability to infect and lyse a variety of malignant tumors, making them potentially useful as therapeutic agents.⁵⁻¹² Several early clinical trials have suggested that these attenuated viruses may be safe for clinical application.¹³⁻¹⁵ Our group has described the construction of a series of replication-competent, attenuated viruses (NV1020 series) based on HSV-1 that have potent antitumoral effects in animal models.^{16,17} Although these viruses were not specifically designed to target malignant tumors, we have repeatedly observed that they display a remarkable selectivity for infecting malignant cells over normal cells.¹⁸⁻²⁰ Historical studies have suggested that HSV-1 has a natural tropism for infecting malignant tumors, although the mechanism for this remains unclear.^{21,22} We have also noted that there may be significant variation in the sensitivity of different cancer cell lines to viral infection, replication, and cell lysis by oncolytic HSV.¹¹⁻¹² These observations have led to our current goal of defining the tumor cell factors that account for sensitivity to oncolytic herpes viral infection, viral replication, and cell lysis. Such information may help to elucidate why some tumors are highly sensitive to oncolytic HSV, and may lead to methods of selecting patients with the most sensitive tumors for HSV therapy.

A critical step in the life cycle of HSV-1 is the attachment and entry by a viral particle into a host cell. Successful HSV infection of susceptible cells depends upon interactions between a viral particle and cell surface receptors required for viral entry.²³ Initially, HSV glycoproteins B and C, which project outward from the viral envelope, attach to heparan sulfate proteoglycans present on cell membrane surfaces. Following this attachment, HSV envelope glycoprotein D (gD) interacts with one of three known cell membrane receptors that are necessary for successful viral fusion with the cell membrane and subsequent viral entry. These gD receptors include herpes viral entry mediator (HVEM), nectin-1, and 3-O-sulfated heparan sulfate (3-OS-HS).²³ HVEM is a member of the tumor necrosis receptor family, nectin-1 belongs to the immunoglobulin superfamily, and 3-OS-HS is a form of heparan sulfate modified by D-glucosaminyl 3-O-sulfotransferase.²⁴⁻²⁶ After interactions between HSV gD and cell surface receptors, the HSV glycoproteins

Correspondence: Richard J Wong, Head and Neck Service, C-1069, Memorial Sloan-Kettering Cancer Center, 1275 York Avenue, New York, New York 10021, USA. E-mail: wongr@mskcc.org

B, H, and L form a complex that mediates fusion of the herpes viral envelope with the cell membrane, leading to viral entry into the host cell. Of the steps involved in viral entry, interactions between viral gD with cellular gD receptors are considered critical in determining successful viral entry.²³

Our goal was to determine if an assessment of HSV receptor expression on cancer cells can be used to predict response to oncolytic HSV therapy. We demonstrate that the density of cell surface nectin-1, a gD receptor, is highly correlated statistically with NV1023 entry, replication, and cytotoxicity. Furthermore, we show that tumor nectin-1 correlates with response to NV1023 therapy *in vivo*, and may be qualitatively measured with immunohistochemistry (IHC). The assessment of tumor nectin-1 may have clinical applicability in selecting patients with high expressing tumors for entry into upcoming clinical trials with oncolytic HSV. Interestingly, we also found that nectin-1 expression and HSV susceptibility were inversely correlated with E-cadherin expression, suggesting that tumors lacking E-cadherin might be particularly appropriate targets for oncolytic HSV therapy.

RESULTS

Viral entry assays

NV1023 expresses the *Escherichia coli lacZ* gene under the control of an immediate early $\alpha 47$ promoter. Viral entry by NV1023 into each head and neck squamous carcinoma (HNSCC) cell line was assessed by lacZ assay. Measured levels of β -galactosidase ranged from 0.1 to 2.2 MU at 6 h, 0.6 to 5.1 MU at 9 h, and 1.9 to 12.6 MU at 12 h following exposure to NV1023 at multiplicity of infection (MOI) 5 (**Figure 1a**). At 9 h, MSKQLL2 (5.1 MU) was most susceptible to viral entry, whereas MDA1386 (0.6 MU) was most resistant. These ranges demonstrate significant variation in permissiveness to early viral entry by different HNSCC lines. The control CHOK1 cell line, which lacks nectin-1 or HVEM expression, allowed no detectable viral entry.

Viral plaque assays

Efficacy of NV1023 replication within the panel of HNSCC was assessed. Viral replication was measured by plaque assay after infection with NV1023 at MOI 1. A wide range of viral titers was detected, ranging from a low of 1,400 PFU for MDA1386, up to a high of 2.1×10^6 PFU by MSKQLL2 (**Figure 1b**). This variation demonstrates innate differences in the ability of HNSCC to support NV1023 replication. The CHOK1 cell line yielded the lowest measured level of viral plaques at just 1,100 PFU, likely representing residual virus from the initial inoculum of NV1023.

Cytotoxicity assays

Viral cytotoxicity in HNSCC was assessed by lactate dehydrogenase assay following infection of HNSCC with NV1023 at MOI 1 and 5 (**Figure 1c and d**). At MOI 5, all cell lines demonstrated nearly complete cell lysis by day 6, showing that at sufficient doses, NV1023 is able to effectively lyse all of these HNSCC. At MOI 1, there was variability in response. By day 6, nearly 40% of MDA1386 cells remained viable, in contrast to just 5% of MSKQLL2 cells. The CHOK1 cell line was the most resistant cell line, with no detectable cytotoxicity at MOI 5.

S-phase fraction and doubling time

Previous studies have demonstrated that the G207 HSV, lacking the ribonucleotide reductase gene, replicates more efficiently in rapidly dividing cells.^{2,8} In contrast, NV1023 has intact ribonucleotide reductase and may not necessarily replicate in such a preferential fashion. To assess possible relationships between cell growth rates and viral susceptibility, HNSCC in logarithmic phase growth were subjected to cell cycle analysis and proliferation studies to determine S-phase fractions and doubling times (**Figure 2a and b**). S-phase fractions varied from 7.9% for MSKQLL1 to 38.1% for SCC1483. Doubling times varied from 43.7 h for MDA1386 to 93.9 h for MSK922. The CHOK1 cell line was the most rapidly dividing cell line, with an S-phase fraction of 42.4% and a doubling time of 22.6 h.

Nectin-1, HVEM and total gD receptor assessment

HNSCC expression of surface nectin-1 and HVEM receptors was assessed by quantitative fluorescence-activated cell sorting (qFACS; **Figure 2c and d**). The average number of antibody binding sites (ABS) per cell corresponds to the number of receptors. Nectin-1 expression varied widely from a low of 17,389 ABS (MDA1386), to a high of 494,906 ABS (MSKQLL2). In contrast, HVEM showed a much lower level of expression and variation, ranging from 569 ABS (MSKQLL1) to 1958 ABS (MDA1986). The CHOK1 cell line showed essentially undetectable nectin-1 (89 ABS) and a low level of HVEM (981 ABS). The low level of HVEM measured likely reflects nonspecific binding by the HVEM antibody used, as CHOK1 cells are devoid of nectin-1 and HVEM receptors. Cellular ELISA (cELISA) was performed as a composite measure of total gD expression using a soluble gD:Fc fusion protein (**Figure 2e**). This assay measures a composite of nectin-1, HVEM, and 3-OS-HS binding sites. The optical density readings from this assay were within a small range, varying from 0.31 (MSKQLL1) to 0.43 (SCC15). The CHOK1 cell line exhibited the lowest total gD receptor expression with an optical density of 0.27.

Statistical correlations

Viral sensitivity data (viral entry, replication, and cytotoxicity) were compared with S-phase, doubling time, and cell surface receptor data to identify significant associations. There were no correlations identified between S-phase (**Figure 3a**) or doubling time (**Figure 3b**) with any of the three sensitivity parameters, indicating that host cell replication rate is not a determinant of NV1023 susceptibility. Nectin-1 expression was strongly and significantly correlated with all three measures of NV1023 sensitivity (**Figure 3c**). Pearson's coefficients were 0.85 for viral entry, 0.79 for viral replication, 0.83 for cytotoxicity at MOI 1, and 0.85 for cytotoxicity at MOI 5; all four correlations were significant ($P < 0.05$). In contrast, HVEM expression did not correlate with any measure of NV1023 sensitivity (**Figure 3d**). cELISA measurements of total gD receptor expression also demonstrated significant correlations, although slightly weaker than nectin-1 (**Figure 3e**). Significant Pearson's coefficients for total gD receptor expression were 0.75 for viral entry and 0.78 for cytotoxicity at MOI 1.

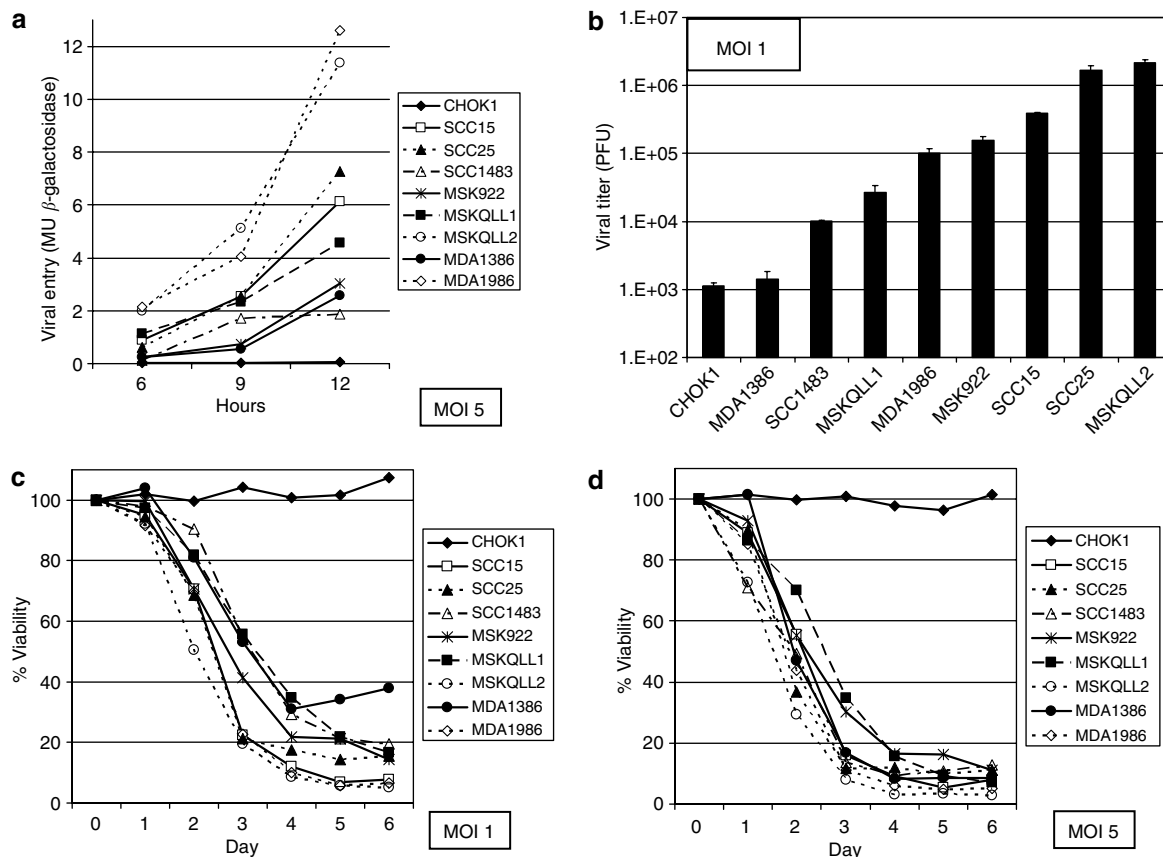


Figure 1 Sensitivity of a panel of HNSCC to NV1023, an oncolytic HSV-1. Viral entry was measured by lacZ assays at MOI 5 (**a**), viral replication by plaque assays at MOI 1 (**b**, logarithmic scale, error bars indicate standard error of mean), and viral cytotoxicity by lactate dehydrogenase assays at MOI 1 (**c**) and MOI 5 (**d**). Variation in response across these cell lines was noted with all three measures of viral sensitivity. MSKQLL2 was the most sensitive to all three parameters, whereas MDA1386 was the least sensitive of the HNSCC. The control CHOK1 cell line that does not express nectin-1 or HVEM was highly resistant to all measures of sensitivity.

Receptor blocking assays

Antibody blocking studies of NV1023 viral entry were performed to corroborate differences between the relative importance of nectin-1 and HVEM receptor function by HNSCC. There were dose-dependent responses seen between nectin-1 antibody concentrations and the degree of viral entry inhibition. The efficacy of antibody blockade of viral entry into cancer cell lines generally corresponded with the level of nectin-1 expression (**Figure 2c**). At a nectin-1 antibody concentration of 100 μ g/ml, viral entry averaged 37% that of unblocked HNSCC for the entire group, ranging from 13% (MSKQLL2) to 62% (MDA1386, **Figure 4a**). These two cell lines allowed the highest and lowest unblocked viral entry (**Figure 1a**) and showed the highest and lowest nectin-1 expression (**Figure 2c**). In contrast, HVEM receptor blockade had a lesser effect on impeding viral entry (**Figure 4b**). At an HVEM antibody concentration of 100 μ g/ml, viral entry averaged 71% that of unblocked HNSCC, ranging from 53% (SCC15) to 88% (MDA1386). Recognizing that these findings are dependent on the characteristics of the antibodies used, these data suggest that nectin-1 receptors may play a greater role than HVEM receptors in NV1023 viral entry into HNSCC.

Nectin-1 transfections

Transient transfections using varying doses of a nectin-1 plasmid (pBG38) were performed on MDA1386, the lowest nectin-1 expressing cancer cell line, and viral entry of NV1023 was assessed by lacZ assays. Increasing levels of nectin-1 expression with increasing doses of transfected pBG38 were observed by Western blot (**Figure 4c**). Viral entry following pBG38 transfections demonstrated a dose-response relationship with increased viral entry associated with higher doses of pBG38 (**Figure 4c**). At the highest dose of transfected pBG38 tested (3 μ g), viral entry was increased 4-fold as compared with non-transfected controls.

Murine Flank tumor therapy and X-gal histochemistry

NV1023 therapy of established murine flank tumors was performed to determine if measured differences in nectin-1 expression by HNSCC correspond to differences in clinical response *in vivo*. Three HNSCC were selected with varying nectin-1 expression: MSKQLL1 (low: 88,925 ABS), MDA1986 (moderate: 162,139 ABS), and SCC15 (high: 298,618 ABS). Tumors excised 24 h after intratumoral injection with NV1023 at 2×10^7 PFU demonstrated mild (MSKQLL1), moderate (MDA1986), and intense (SCC15) lacZ staining corresponding

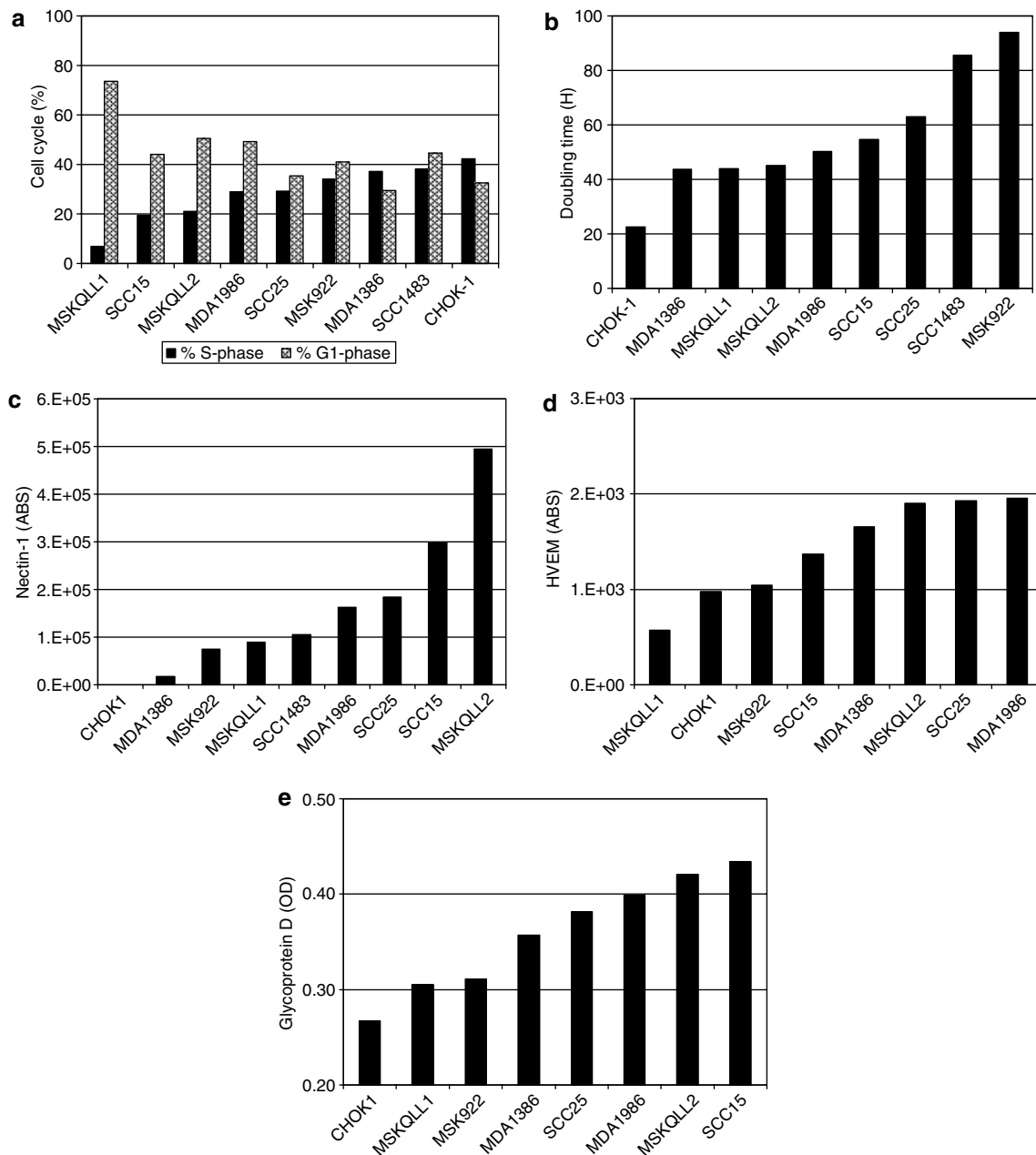


Figure 2 Potential determinants of NV1023 sensitivity in HNSCC. HNSCC underwent cell cycle analysis for S-phase fraction (**a**) and determination of doubling time (**b**). Quantitative FACS was performed for assessment of cell surface nectin-1 (**c**) and HVEM (**d**) expression as measured by the number of ABS (ABS), or the average number of receptor sites per cell. Nectin-1 expression exhibits significant variation between the different HNSCC, whereas HVEM expression falls within a narrower range. cELISA using a soluble fusion gD:Fc protein was performed to assess for total gD expression (**e**) as measured by optical density (OD) with spectrophotometry.

with nectin-1 expression (**Figure 5a**). SCC15 showed the greatest response with a reduction of tumor volume to just 4% of control tumors, followed by MDA1986 at 17% and MSKQLL1 at 26% by day 18 (**Figure 5b** and **c**). These results suggest that variance in nectin-1 expression may correspond to clinically relevant differences in tumor response to oncolytic HSV therapy *in vivo*.

Nectin-1 and E-cadherin IHC

IHC was performed to determine if nectin-1 could be assessed on fresh tumor tissues; such a technique could facilitate rapid

nectin-1 assessment of patient biopsy specimens in clinical practice. IHC for nectin-1 was interpreted by a blinded pathologist and qualitatively confirmed qFACS data of nectin-1 expression. There was strongly positive nectin-1 staining in HNSCC with higher qFACS nectin-1 levels (>162,000 ABS), and there was low staining for HNSCC with lower qFACS nectin-1 levels (<89,000 ABS; **Figure 6**). Small differences in nectin-1 expression measured by qFACS were not measurable by IHC. As nectin-1 and E-cadherin both form components of intercellular adherens junctions, we

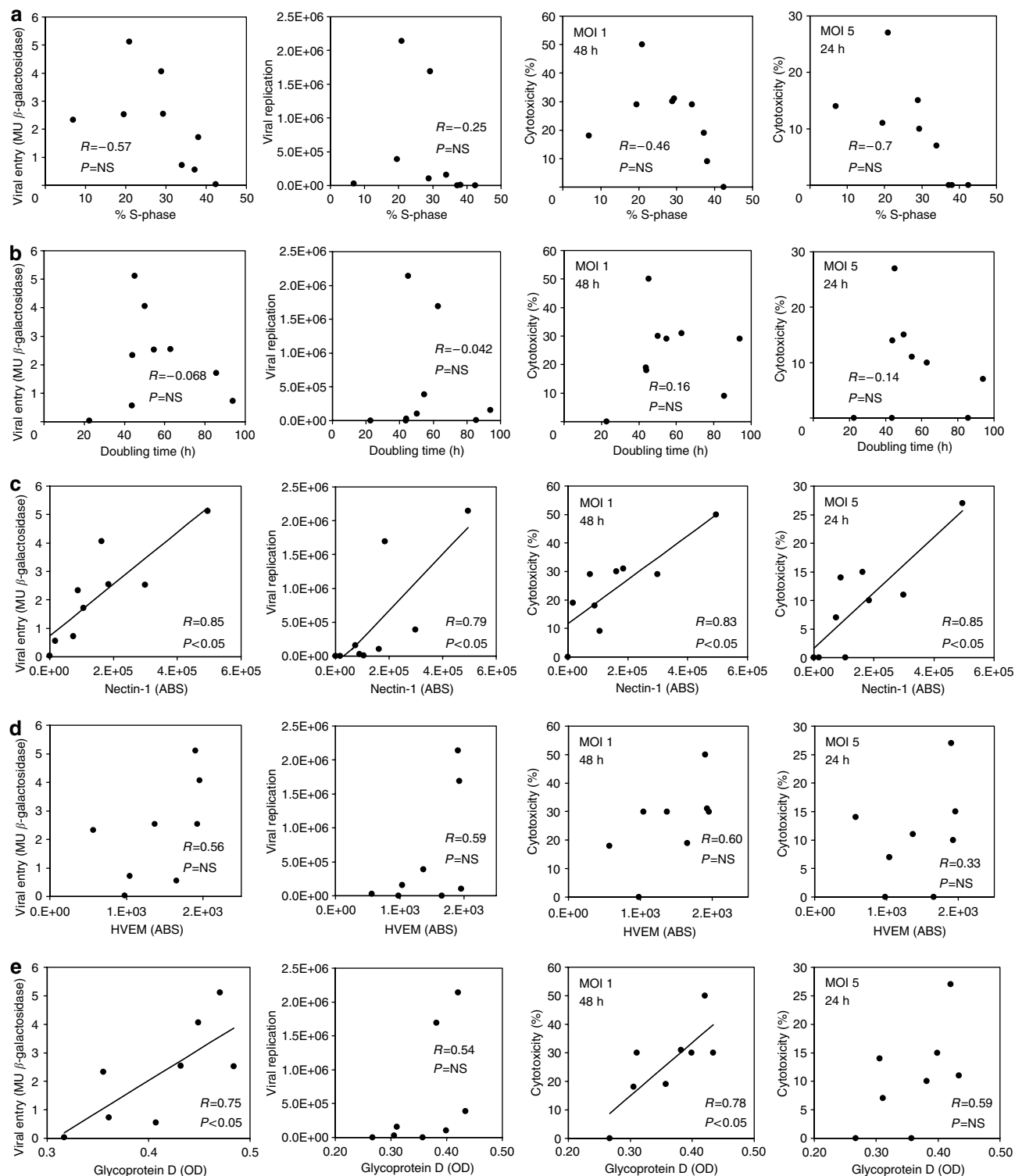


Figure 3 Pearson's coefficients comparing measures of NV1023 sensitivity (viral entry at 9 h, viral replication and cytotoxicity at MOI 5, 24 h, and MOI 1 for 48 h) with potential cellular determinants of sensitivity. Doubling time (**a**), S-phase fraction (**b**), and HVEM expression (**d**) show no correlations with any of the viral sensitivity measures. Nectin-1 expression (**c**) was significantly correlated with all measures of sensitivity, with R -values of 0.8 or greater for each parameter ($P < 0.05$ for all). Total gD receptor expression showed significant correlations with viral entry ($R = 0.75$) and cytotoxicity at MOI 1 ($R = 0.78$), although correlations with viral replication and cytotoxicity at MOI 5 did not show significance.

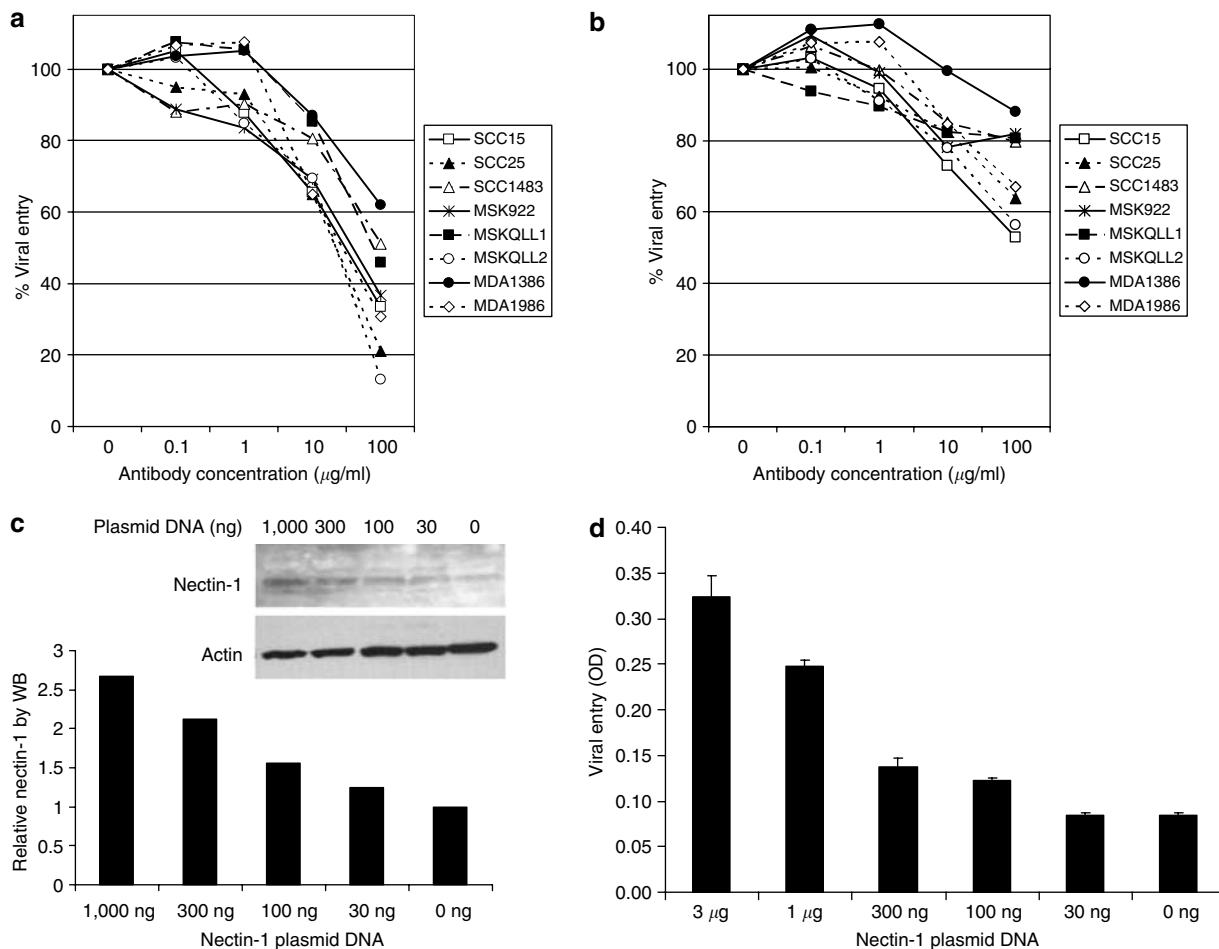


Figure 4 Effects of inhibition and enhancement of tumor nectin-1 on viral entry. LacZ assays were performed to assess NV1023 viral entry into HNSCC with or without the addition of nectin-1 or HVEM blocking antibodies at varying concentrations. Higher concentrations of nectin-1 antibody led to progressively decreased viral entry. Anti-nectin-1 antibodies (R1.302.12) at 100 µg/ml impeded viral entry by NV1023 by an average of 37% (range 13–62%) as compared to nonblocked HNSCC (a). In contrast, anti-HVEM antibodies (CW10) at 100 µg/ml decreased viral entry to an average of 71% (range 53–88%) as compared to nonblocked HNSCC (b). Nectin-1 appears to play a greater functional role in permitting NV1023 viral entry. Nectin-1 transfections of the lowest nectin-1 expressing cancer cell line (MDA1386) were performed using varying amounts of nectin-1 plasmid DNA (pBG38), and Western blots were performed to confirm increased protein expression with increasing amounts of pBG38 transfection (c). Viral entry into nectin-1-transfected MDA1386 cells was assessed with lacZ assays after exposure to NV1023 at MOI 5 for 6 h (d). A dose-response relationship between amount of pBG38 transfected and viral entry is seen, with a 4-fold increase in viral entry at the highest (3 µg) dose of pBG38 transfected.

hypothesized that a loss of E-cadherin in malignant cells might affect the availability of nectin-1. The intensity of E-cadherin staining was found to be inversely related to nectin-1 staining (Figure 6).

DISCUSSION

Replication-competent, attenuated HSV based on HSV-1 have repeatedly demonstrated significant therapeutic effects for a variety of human malignancies in experimental models, with favorable safety profiles in early clinical trials.^{5–15} Some engineered HSV have been designed to target malignant cells through the insertion of tissue-specific promoters driving the HSV $\gamma_{134.5}$ or ribonucleotide reductase genes to promote selective viral replication.^{27–30} However, we have observed that oncolytic HSV without such a tumor-targeting design nonetheless demonstrates a strong selectivity for infecting malignant cells preferentially over benign cells.^{18–20} Historical studies have also shown that wild-type HSV-1 possesses a natural tropism for

infecting tumor tissues.^{21,22} We hypothesized that there may be innate factors in malignant cells that predispose them to infection and lysis by oncolytic HSV-1.

Cells with activated Ras or mitogen-induced extracellular kinase signaling pathways have been shown to have an impaired protein kinase R response to viral infection, allowing permissive viral replication by double $\gamma_{134.5}$ -deleted oncolytic HSV-1.^{31–34} However, this mechanism does not account for our observations of selective early infection *in vivo* by the NV1023 series of viruses, which carry one intact copy of the $\gamma_{134.5}$ gene.^{18–20} We have further observed that cancer cells once infected by NV1023 appear condemned to cell lysis, and measures of viral entry into cancer cells correlate both temporally and quantitatively with measures of cell lysis.^{12,16} We hypothesized that the fate of a target cancer cell is likely to be determined by early events. A key step for successful HSV-1 infection is the attachment and entry of the virus into the host cell. The interactions between HSV gD and cell surface gD receptors (nectin-1, HVEM, and 3-OS-HS)

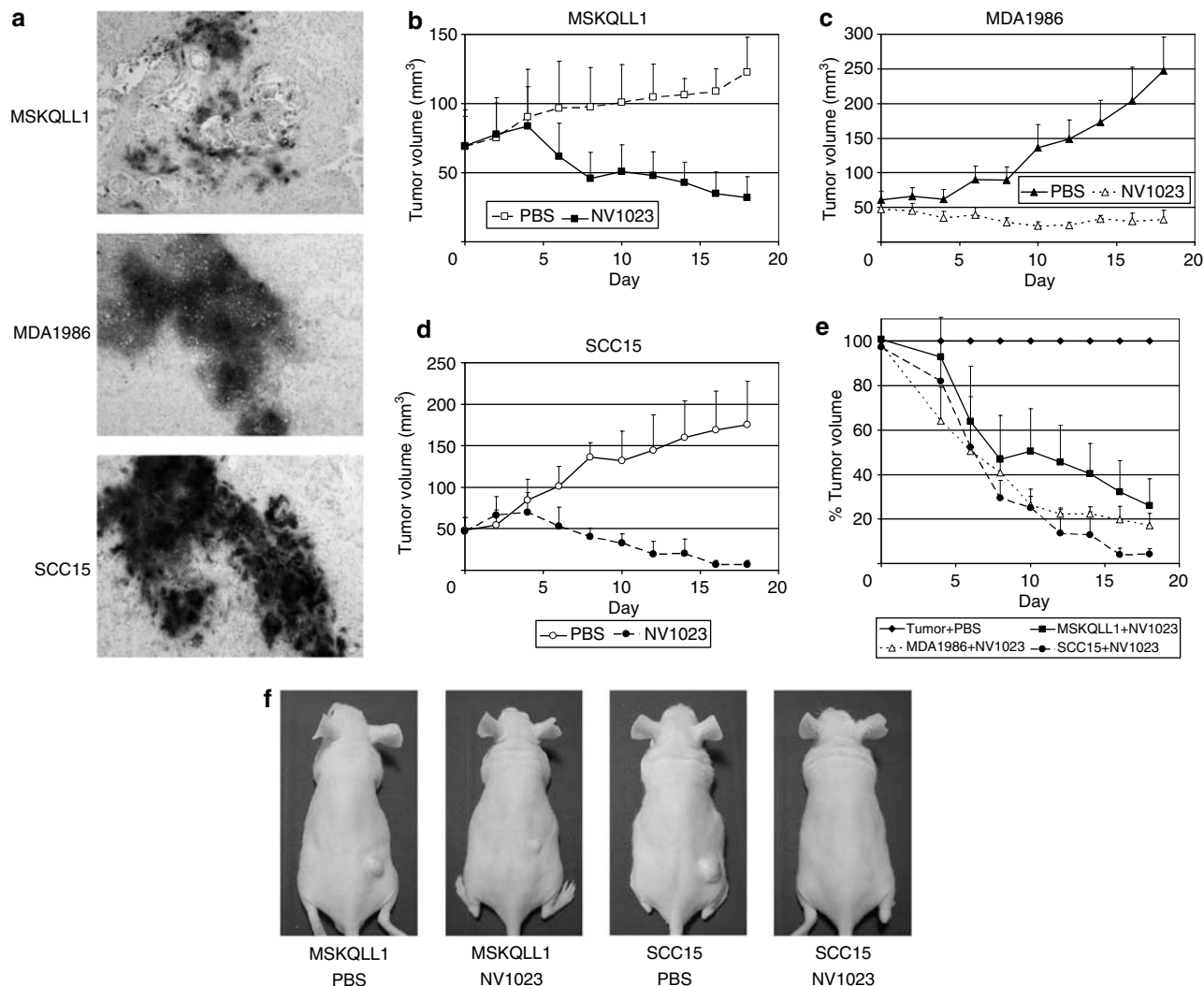


Figure 5 Murine flank tumors of HNSCC with high (SCC15), moderate (MDA1986), and low (MSKQLL1) nectin-1 expression were treated with a single intratumoral injection of NV1023 (2×10^7 PFU). X-gal histochemistry of flank tumors excised at 24 h demonstrates an inverse relationship between nectin-1 level and staining intensity, with progressively greater viral infection in the cell lines with higher nectin-1 expression (**a**). In other animals, tumor volumes were measured over time, and the percentage of tumor volume of treated tumors as compared to untreated, control tumors was calculated (**b-d**, error bars indicate standard error of mean). A comparison of percentage tumor volume reduction between cell lines shows a correlation with nectin-1 expression; SCC15 exhibits the most significant tumor regression, followed by MDA1986 and MSKQLL1 (**e**). Representative flank tumors are shown at day 18 (**f**).

are recognized as critical in determining if a cell can be successfully infected by HSV-1.²³

In addition to functioning as a cell surface receptor for herpesviruses, nectin-1 plays an important role in the normal structure of intercellular adherens junctions, which maintain attachments between adjacent cells.³⁵ Within the adherens junctions, nectin-1 and afadin form intercellular bridges together, as do E-cadherin and β -catenin. The loss of E-cadherin is a well-described mechanism of carcinogenesis that decreases intercellular adhesion and increases potential for invasion and metastases.^{36,37} Interestingly, there is evidence that processes leading to the disruption of adherens junctions may liberate nectin-1 to function as an HSV receptor. Yoon and Spear³⁸ found that directly disrupting adherens junctions through calcium depletion led to an enhanced availability of nectin-1. The

increased cell surface nectin-1 was able to function as a viral receptor, making these cells more susceptible to HSV-1 infection. Using a similar concept, we found that highly invasive squamous carcinoma cell lines with decreased intercellular adhesion expressed higher levels of surface nectin-1 in comparison to less invasive carcinoma lines.³⁹ The increased nectin-1 levels in the highly invasive cell lines acted as functional HSV receptors, permitting enhanced viral entry and cytotoxicity.

The goal of this study was to determine if quantifying nectin-1 expression on a panel of human squamous carcinomas may predict sensitivity to HSV oncolysis. Understanding the determinants of HSV oncolytic sensitivity might allow clinicians to identify patients who are most likely to benefit from therapy with these viruses. We assessed the expression of two HSV-1 gD receptors, nectin-1 and HVEM, using quantitative FACS on a

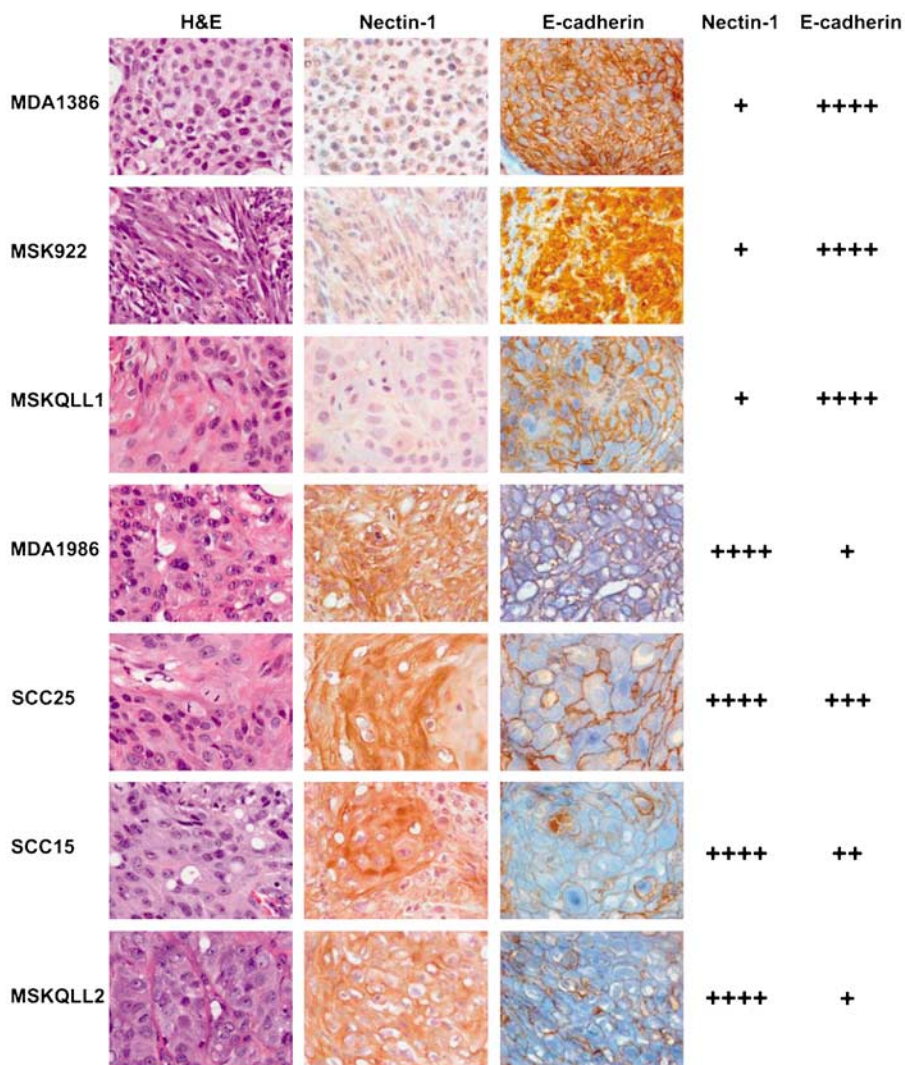


Figure 6 Nectin-1 and E-cadherin IHC, and hematoxylin and eosin (H and E) staining of HNSCC. Three HNSCC (MDA1386, MSK922, MSKQLL1) with lower nectin-1 expression by qFACS ($\leq 88,925$ ABS) are compared to four HNSCC (MDA1986, SCC25, SCC15, MSKQLL2) with higher nectin-1 expression by qFACS ($\geq 162,139$ ABS). Nectin-1 staining qualitatively corroborates qFACS data by distinguishing between high and low expression. Both nectin-1 and E-cadherin are components of intercellular adherens junctions, and processes leading to the disruption of these junctions may enhance nectin-1 availability. E-cadherin staining is inversely correlated with nectin-1, suggesting that the loss of E-cadherin may be associated with enhanced nectin-1 surface expression and oncolytic HSV sensitivity.

panel of human HNSCC. Sensitivity to NV1023 was measured by three parameters: viral entry, viral replication, and viral cytotoxicity. We found strong correlations between nectin-1 and viral entry. Downstream events of viral replication and cytotoxicity were also significantly correlated with nectin-1 expression, underscoring the importance of initial viral entry in determining secondary replicative and oncolytic effects. In contrast, HVEM failed to demonstrate significant correlations. Quantitative FACS ABS values were lower for HVEM than nectin-1, with less variability between different cell lines.

The blockade of nectin-1 on HNSCC led to a greater inhibition of NV1023 viral entry as compared to blockade of HVEM. Recognizing that these observations are dependent on the antibodies used, nectin-1 appears to play a greater role than HVEM for permitting NV1023 entry into HNSCC. Nectin-1 transfection experiments demonstrated that NV1023 viral entry

into the low-nectin-1 expressing MDA1386 cell line could be increased in proportion to the amount of nectin-1 plasmid (pBG38) used for transfections. Established flank tumors treated with NV1023 demonstrated levels of infection and tumor volume response that correlated with nectin-1 expression level. These results suggest that tumor nectin-1 expression may reflect *in vivo* response to NV1023 therapy.

A third gD receptor, 3-OS-HS, could not be quantified directly owing to the lack of an available specific antibody. To account for 3-OS-HS receptor activity, a soluble gD:Fc fusion protein was used as a ligand to measure total gD receptor expression, reflecting a summation of nectin-1, HVEM, and 3-OS-HS expression. cELISA data yielded significant correlations with viral entry and cytotoxicity sensitivity data. These correlations were slightly weaker than the nectin-1 qFACS correlations, suggesting that the additional assessment of HVEM

and 3-OS-HS through this method does not add predictive value. Differences in the status of adherens junctions and nectin-1 availability between these methods may exist, as qFACS measures receptor levels on individual cells in suspension, while cELISA assesses receptor expression on a confluent cell monolayer. We also found that IHC was feasible on tumor sections and could distinguish between tumors with high and low nectin-1 expression.

The loss of E-cadherin provides one mechanism to account for our observations of increased nectin-1 expression and HSV sensitivity by these cancer cell lines. E-cadherin is frequently downregulated in cells that undergo malignant transformation, and the loss of E-cadherin is linked to increased cancer invasiveness and metastatic ability through dysfunction of adherens junctions.^{36,37} As processes disrupting adherens junctions such as calcium depletion may enhance nectin-1 exposure and HSV susceptibility,³⁸ we hypothesized that HNSCC with decreased E-cadherin and adherens junctions function might also have increased surface nectin-1. Our results support this concept by showing a strong inverse relationship between nectin-1 and E-cadherin expression. These findings suggest that highly invasive and metastatic tumors lacking E-cadherin might be particularly sensitive targets for oncolytic HSV-1 therapy.

In summary, we demonstrate that tumor nectin-1 expression may be assessed by qFACS and IHC, and that this assessment is predictive of NV1023 therapeutic response. These findings provide (1) a mechanism to account for variation in tumor sensitivity to oncolytic HSV, and (2) a simple method to identify patients with the most sensitive tumors for therapy with oncolytic HSV. E-cadherin-deficient cancers appear to have higher nectin-1 expression, and might be particularly appropriate targets for therapy. In the future, nectin-1 assessment of tumor biopsy specimens might facilitate optimal selection of patients for entry into future clinical trials with these promising vectors.

MATERIALS AND METHODS

Cell lines. Eight human HNSCC cell lines were studied: SCC15, SCC25, SCC1483, MSK922, MSKQLL1, MSKQLL2, MDA1386, and MDA1986. CHOK1 is devoid of surface nectin-1 and HVEM, and was used as a control (gift of Dr Patricia Spear, Northwestern University). MDA1386 was grown in Rosewell's Park Memorial Institute media with 10% fetal calf serum (FCS) and 1% P and S CHOK1 was grown in F12 with 10% FCS and 1% P and S. All other cell lines were grown in MEM containing 10% FCS and 1% P and S.

Virus. We described the construction of NV1023, an attenuated, replication-competent, oncolytic herpesvirus.¹⁶ NV1023 was derived from R7020, an HSV-1 originally designed as a vaccine candidate.^{3,4,11} NV1023 carries a 5.2-kb fragment of HSV-2 DNA, containing HSV-2 genes US2-2 to US2-5, inserted in the UL/S junction.¹⁶ NV1023 is attenuated by a 15-kb deletion in the inverted repeat region that extends from the 3' end of UL55 to the promoter for ICP4, deleting UL56 and one copy of the diploid genes ICP0, ICP4, and γ_1 34.5. NV1023 also contains the *Escherichia coli* β -galactosidase gene inserted at the US10-12 locus under control of the α 47 promoter and expresses wild-type HSV-1 envelope glycoproteins. NV1023 was provided by MediGene (San Diego, CA).

Viral entry assays. Viral entry by NV1023 was measured by assessment of lacZ expression using the enhanced β -galactosidase assay kit (Gene Therapy Systems, San Diego, CA). Cells (4×10^4) were plated in 96-well plates in 100 μ l media. After 6 h, NV1023 in 50 μ l phosphate-buffered saline (PBS) was added at MOI 5. At 6, 9, and 12 h, media were aspirated and lysis buffer was added. Serial dilutions of lacZ were used to create a standard reference curve. Substrate was added and plates were read on a spectrophotometer at 570 nm. Three replicate samples were performed for each condition.

Plaque assays. Cells (2×10^4) were plated in 12-well plates in 1 ml media. After 6 h, NV1023 (100 μ l) was added to each well at MOI 1. The supernatant was collected at 48 h. Serial dilutions were added to confluent Vero cells for 4 h. Wells were washed with media and covered with 1% agarose with media. After 48 h, 2 ml of neutral red solution (2% by volume) was added and viral plaques were counted after 24 h. Three replicate samples were performed for each condition.

Cytotoxicity assays. Cells (2×10^4) were plated in 12-well plates in 1 ml media. After 6 h, NV1023 in 100 μ l PBS was added to each well at MOI 0, 1, and 5. At daily intervals, cells were washed with PBS and lysed with Triton X (1.35%) to release intracellular lactate dehydrogenase, which was quantified with a Cytotox 96 kit (Promega, Madison, WI) and spectrophotometry (EL321e, Bio-Tek Instruments, Winooski, VT) at 450 nm. On day 4, an additional 1 ml of fresh media was added to the remaining wells. Results were expressed as the percentage of surviving cells determined from comparing test samples to untreated samples. Three replicate samples were performed for each condition.

Cell cycle and doubling time. Cells at 70–80% confluence were trypsinized and suspended in NP-40 solution (10 mM NaCl, 3.4 mM sodium citrate, 0.03% NP-40, 63 μ M ethidium bromide, 10 μ g RNaseA/ml) at 1×10^6 cells per ml. After 1 h at room temperature, equal volume of high-sucrose ethidium bromide solution was added (0.25 M sucrose, 78 mM citric acid, 100 μ M ethidium bromide). The DNA content was determined on a FACScalibur flow cytometer. Cell proliferation was measured by plating 2×10^4 cells in six-well plates with 3 ml media. Wells were trypsinized daily, stained with Trypan blue and counted to determine the number of viable cells.

Quantitative fluorescence-activated cell sorting. Microbeads (Quantum Simply Cellular, Sigma-Aldrich, St Louis, MO) were used as a standard reference for determining the number of ABS or receptor numbers on cell lines.⁴⁰ Mouse monoclonal antibodies CW10 (anti-HVEM, Santa Cruz, Santa Cruz, CA) and R1.302.12 (anti-nectin-1, Beckman Coulter, Fullerton, CA) conjugated with phycoerythrin were used. R1.302.12 has been well characterized for its nectin-1 specificity, although CW10 is less well characterized. Cells were suspended in PBS with 3% FCS and 0.01% sodium azide. Antibodies were diluted to concentrations found to be sufficient to saturate cell surface binding of the SCC15 and QLL2 cell lines. Antibodies were added to 3×10^5 cells and incubated on ice for 1 h. Microbeads were processed identically as test samples. Samples were washed with PBS-FCS, fixed with 3% paraformaldehyde, and run on a FACScaliber flow cytometer (Becton Dickinson, Franklin Lakes, NJ). Data were analyzed using FlowJo software version 6.0 (Tree Star, Ashland, OR).

Soluble gD:Fc fusion protein cELISA. Plasmid for a gD:Fc soluble fusion protein (Dr Patricia Spear, Northwestern University) was used to transfect CHO-K1 cells using lipofectamine (Invitrogen, Carlsbad, CA). The supernatant was collected at 48 h, clarified by centrifugation, and gD:Fc protein quantified using an anti-rabbit IgG ELISA kit

(Alpha Diagnostic International, San Antonio, TX). Cells (1×10^5) were seeded in 96-well plates, fixed with 2% formaldehyde and 0.2% glutaraldehyde, and incubated with 50 μ l of gD:Fc protein (1 μ g/ml) for 1 h at room temperature. Cells were then exposed to a biotinylated, anti-rabbit IgG secondary antibody (1:1,000, Chemicon, Temecula, CA) for 30 min, followed by streptavidin-conjugated horseradish peroxidase (1:20,000, Amersham Biosciences, Piscataway, NJ) for 30 min. Substrate was added (T-5525, P4922, Sigma-Aldrich) and plates were read on a spectrophotometer at 370 nm. The assay was performed on four replicate samples for each condition.

Receptor blocking assays. The viral entry assay was modified for receptor blocking assays. The 96-well plate was chilled on ice. Mouse monoclonal antibodies CW10 (anti-HVEM) and R1.302.12 (anti-nectin-1) were serially diluted to 0.01, 0.1, 1, 10, and 100 μ g/ml in 50 μ l media. An equal volume of NV1023 virus diluted in culture medium at MOI 5 was added and cells were placed at 37°C for 6 h. β -Galactosidase activity was measured as described above. Data are expressed as the percentage of viral entry under antibody blockade as compared to under unblocked conditions.

Nectin-1 transfections. Nectin-1 transfections were performed on MDA1386 using the pBG38 nectin-1 plasmid (Dr Claude Krummenacher, University of Pennsylvania). Subconfluent cells were transfected with 3 μ g, 1 μ g, 300 ng, 100 ng, 30 ng and 0 ng of pBG38 per well in six-well plates. Plasmid pUC19 was used as carrier DNA to bring the total DNA amount to 3 μ g/well. DNA was mixed with GenePORTER (Gene Therapy Systems, 15 μ l/well) in 1 ml/well of serum-free DMEM for 30 min at room temperature. This mixture was added to cells for 3.5 h at 37°C and then 1 ml of DMEM with 20% FCS was added for 40 h. Cells were seeded on 96-well plates for viral entry assays using NV1023 (MOI 5, 6 h) or centrifuged for Western blot.

Western blots. Cell pellets were sonicated for 10 s and clarified by centrifugation. Total protein (20 μ g) underwent electrophoresis in 10% Tris-HCl gels (Bio-Rad), were transferred to polyvinylidene difluoride membranes, blocked, and exposed to a goat polyclonal nectin-1 primary antibody (C-20, 1:200, Santa Cruz) or actin antibody (C-11, 1:200, Santa Cruz) followed by a secondary antibody conjugated to horseradish peroxidase. Bands were developed using an ECL Plus detection system (Amersham). Density was quantified (AlphaImager Imaging Systems, Alpha Innotech, San Legndra, CA), and the nectin-1 expression of each sample was divided by its control actin level to yield a relative expression level.

Murine Flank tumor therapy. Six-week-old athymic nude mice (National Cancer Institute) were anesthetized with inhalational methoxyflurane. Tumors were established for MSKQLL1, MDA1986, and SCC15 by injecting 2×10^6 cells in 50 μ l of PBS into the subcutaneous flanks of athymic nude mice. When tumors had reached approximately 5 mm, flank tumors ($n = 5$ per group) were treated by a single dose of NV1023 (2×10^7 PFU) or PBS. Tumor dimensions were serially measured and volumes calculated by the following formula: ellipsoid volume = $(4/3)\pi(\text{length}/2)(\text{width}/2)^2$.

X-gal histochemistry. Established flank tumors of MSKQLL1, MDA1986, and SCC15 were injected with NV1023 at 2×10^7 PFU. After 24 h, animals were killed, and flank tumors were excised, frozen in Tissue Tek solution and cut into sections 8 μ m thick. Slides were fixed with 1% glutaraldehyde for 5 min, washed with PBS, and stained with X-gal (1 mg/ml) in an iron solution of 5 mM $K_4Fe(CN)_6$, 5 mM $K_3Fe(CN)_6$, and 2 mM $MgCl_2$ at 37°C for 2 h. Slides were counterstained with nuclear fast red.

Nectin-1 and E-cadherin IHC. Established murine flank tumors were excised 14 days after injection, frozen in Tissue Tek, and cut into 8- μ m-thick sections on glass slides. Portions of tumor were fixed in formalin, embedded in paraffin, and stained with hematoxylin and eosin. Slides were fixed with 2% formaldehyde and 0.2% glutaraldehyde, quenched, blocked, and incubated with primary antibody (nectin-1, 1:200, Santa Cruz; E-cadherin, 1:250, BD Transduction Labs, Lexington, KY) overnight at 4°C. Slides were incubated with a biotinylated secondary antibody and visualized with an avidin-biotin complex kit (Santa Cruz). Slides were counterstained with hematoxylin and reviewed in a blinded fashion by a pathologist (RAG).

ACKNOWLEDGMENTS

We thank Patricia Spear (Northwestern University) for her helpful advice and generous provision of the gD:Fc soluble fusion protein plasmid. We also thank Claude Krummenacher (University of Pennsylvania) for his helpful advice regarding the qFACS technique and for his generous provision of the pBG38 plasmid. Presented in part as a poster at the American Association for Cancer Research Annual Meeting, April 18, 2005, Anaheim, CA, USA. RJW was supported by a Clinical Innovator Award from the Flight Attendant Medical Research Institute, and a Faculty Career Development Award from the American College of Surgeons and the American Head and Neck Society.

REFERENCES

- Martuza, RL, Malick, A, Markert, JM, Ruffner, KL and Coen, DM (1991). Experimental therapy of human glioma by means of a genetically engineered virus mutant. *Science* **252**: 854-856.
- Mineta, T, Rabkin, SD, Yazaki, T, Hunter, WD and Martuza, RL (1995). Attenuated multi-mutated herpes simplex virus-1 for the treatment of malignant gliomas. *Nat Med* **1**: 938-943.
- Meignier, B, Longnecker, R and Roizman, B (1988). *In vivo* behavior of genetically engineered herpes simplex viruses R7017 and R7020: construction and evaluation in rodents. *J Infect Dis* **158**: 602-614.
- Meignier, B, Martin, B, Whitley, RJ and Roizman, B (1990). *In vivo* behavior of genetically engineered herpes simplex viruses R7017 and R7020. II. Studies in immunocompetent and immunosuppressed owl monkeys (*Aotus trivirgatus*). *J Infect Dis* **162**: 313-321.
- Toda, M, Rabkin, SD and Martuza, RL (1998). Treatment of human breast cancer in a brain metastatic model by G207, a replication-competent multimitated herpes simplex virus 1. *Hum Gene Ther* **9**: 2177-2185.
- Walker, JR, McGeagh, KG, Sundaresan, P, Jorgensen, TJ, Rabkin, SD and Martuza, RL (1999). Local and systemic therapy of human prostate adenocarcinoma with the conditionally replicating herpes simplex virus vector G207. *Hum Gene Ther* **10**: 2237-2243.
- Coukos, G, Makrigiannakis, A, Kang, EH, Rubin, SC, Albelda, SM and Molnar-Kimber, KL (2000). Oncolytic herpes simplex virus-1 lacking ICP34.5 induces p53-independent death and is efficacious against chemotherapy-resistant ovarian cancer. *Clin Cancer Res* **6**: 3342-3353.
- Kooby, DA, Carew, JF, Halterman, MW, Mack, JE, Bertino, JR, Blumgart, LH and Federoff et al. (1999). Oncolytic viral therapy for human colorectal cancer and liver metastases using a multi-mutated herpes simplex virus type-1 (G207). *FASEB J* **13**: 1325-1334.
- Toyoizumi, T, Mick, R, Abbas, AE, Kang, EH, Kaiser, LR and Molnar-Kimber, KL (1999). Combined therapy with chemotherapeutic agents and herpes simplex virus type 1 ICP34.5 mutant (HSV-1716) in human non-small cell lung cancer. *Hum Gene Ther* **10**: 3013-3029.
- McAuliffe, PF, Jarnagin, WR, Johnson, P, Delman, KA, Federoff, H and Fong, Y (2000). Effective treatment of pancreatic tumors with two multimitated herpes simplex oncolytic viruses. *J Gastrointest Surg* **4**: 580-588.
- Wong, RJ, Kim, SH, Joe, JK, Shah, JP, Johnson, PA and Fong, Y (2001). Effective treatment of head and neck squamous cell carcinoma by an oncolytic herpes simplex virus. *J Am Coll Surg* **193**: 12-21.
- Yu, Z, Eisenberg, DP, Singh, B, Shah, JP, Fong, F and Wong, RJ (2004). Treatment of aggressive thyroid cancer with an oncolytic herpes virus. *Int J Cancer* **112**: 525-532.
- Markert, JM, Medlock, MD, Rabkin, SD, Gillespie, GY, Todo, T and Hunter, WD et al. (2000). Conditionally replicating herpes simplex virus mutant, G207 for the treatment of malignant glioma: results of a phase I trial. *Gene Ther* **7**: 867-874.
- Rampling, R, Cruickshank, G, Papanastassiou, V, Nicoll, J, Hadley, D and Brennan, D et al. (2000). Toxicity evaluation of replication-competent herpes simplex virus (ICP 34.5 null mutant 1716) in patients with recurrent malignant glioma. *Gene Ther* **7**: 859-866.
- Fong, Y, Kemeny, N and Jarnagin, W et al. (2002). Phase 1 study of a replication-competent herpes simplex oncolytic virus for treatment of hepatic colorectal metastases. *Am Soc Clin Oncol Ann Meeting* **27**: Ba.
- Wong, RJ, Patel, SG, Kim, S, DeMatteo, RP, Malhotra, S and Bennett, JJ et al. (2001). Cytokine gene transfer enhances herpes oncolytic therapy in murine squamous cell carcinoma. *Hum Gene Ther* **12**: 253-265.

17. Wong, RJ, Joe, JK, Kim, SH, Shah, JP, Horsburgh, B and Fong, Y (2002). Oncolytic herpesvirus effectively treats murine squamous cell carcinoma and spreads by natural lymphatics to treat sites of lymphatic metastases. *Hum Gene Ther* **13**: 1213-1223.
18. Wong, RJ, Chan, MK, Yu, Z, Kim, TH, Bhargava, A and Stiles, BM *et al.* (2004). Effective intravenous therapy of murine pulmonary metastases with an oncolytic herpes virus expressing interleukin 12. *Clin Cancer Res* **10**: 251-259.
19. Stiles, BM, Bhargava, A, Adusumilli, PS, Stanziale, SF, Kim, TH and Rusch, VW *et al.* (2003). The replication-competent oncolytic herpes simplex mutant virus NV1066 is effective in the treatment of esophageal cancer. *Surgery* **134**: 357-364.
20. Stiles, BM, Adusumilli, PS, Bhargava, A, Stanziale, SF, Kim, TH and Chan, MK *et al.* (2006). Minimally invasive localization of oncolytic herpes simplex viral therapy of metastatic pleural cancer. *Cancer Gene Ther* **13**: 53-64.
21. Levaditi, C and Nicolau, S (1922). Affinité du virus herpétique pour les néoplasmes épithéliaux. *Compt Rend Soc De Biol* **86**: 498-500.
22. Moore, AE (1949). Effect of inoculation of the viruses influenza A and herpes simplex on the growth of transplantable tumors in mice. *Cancer* **2**: 516-524.
23. Spear, PG and Longnecker, R (2003). Herpesvirus entry: an update. *J Virol* **77**: 10179-10185.
24. Montgomery, RI, Warner, MS, Lum, BJ and Spear, PG (1996). Herpes simplex virus-1 entry into cells mediated by a novel member of the TNF/NGF receptor family. *Cell* **87**: 427-436.
25. Geraghty, RJ, Krummenacher, C, Cohen, GH, Eisenberg, RJ and Spear, PG (1998). Entry of alphaherpesviruses mediated by poliovirus receptor-related protein 1 and poliovirus receptor. *Science* **280**: 1618-1620.
26. Shukla, D, Liu, J, Blaiklock, P, Shworak, NW, Bai, X, Esko, JD and Cohen, GH *et al.* (1999). A novel role for 3-O-sulfated heparan sulfate in herpes simplex virus 1 entry. *Cell* **99**: 13-22.
27. Kambara, H, Okano, H, Chiocca, EA and Saeki, Y (2005). An oncolytic HSV-1 mutant expressing ICP34.5 under control of a nectin promoter increases survival of animals even when symptomatic from a brain tumor. *Cancer Res* **65**: 2832-2839.
28. Chung, RY, Saeki, Y and Chiocca, EA (1999). B-myb promoter retargeting of herpes simplex virus gamma34.5 gene-mediated virulence toward tumor and cycling cells. *J Virol* **73**: 7556-7564.
29. Reinblatt, M, Pin, RH, Federoff, HJ and Fong, Y (2004). Utilizing tumor hypoxia to enhance oncolytic viral therapy in colorectal metastases. *Ann Surg* **239**: 892-899.
30. Reinblatt, M, Pin, RH and Fong, Y (2004). Carcinoembryonic antigen directed herpes viral oncolysis improves selectivity and activity in colorectal cancer. *Surgery* **136**: 579-584.
31. Farassati, F, Yang, AD and Lee, PW (2001). Oncogenes in Ras signalling pathway dictate host-cell permissiveness to herpes simplex virus 1. *Nat Cell Biol* **3**: 745-750.
32. Chou, J, Kern, ER, Whitley, RJ and Roizman, B (1990). Mapping of herpes simplex virus-1 neurovirulence to gamma 134.5, a gene nonessential for growth in culture. *Science* **250**: 1262-1266.
33. Chou, J and Roizman, B (1992). The gamma 1(34.5) gene of herpes simplex virus 1 precludes neuroblastoma cells from triggering total shutoff of protein synthesis characteristic of programmed cell death in neuronal cells. *Proc Natl Acad Sci USA* **89**: 3266-3270.
34. Smith, KD, Mezhir, JJ, Bickenback, K, Veerapong, J, Charron, J and Posner, MC *et al.* (2006). Activated MEK suppresses activation of PKR and enables efficient replication and *in vivo* oncolysis by $\Delta\gamma_134.5$ mutants of herpes simplex virus 1. *J Virol* **80**: 1110-1120.
35. Takai, Y, Irie, K, Shimizu, K, Sakisaka, T and Ikeda, W (2003). Nectins and nectin-like molecules: roles in cell adhesion, migration, and polarization. *Cancer Sci* **94**: 655-667.
36. Massarelli, E, Brown, E, Tran, NK, Liu, DD, Izzo, JG and Lee, JJ *et al.* (2005). Loss of E-cadherin and p27 expression is associated with head and neck squamous tumorigenesis. *Cancer* **103**: 952-959.
37. Bosch, FX, Andl, C, Abel, U and Kartenbeck, J (2005). E-cadherin is a selective and strongly dominant prognostic factor in squamous cell carcinoma: a comparison of E-cadherin with desmosomal components. *Int J Cancer* **114**: 779-790.
38. Yoon, M and Spear, PG (2002). Disruption of adherens junctions liberates nectin-1 to serve as receptor for herpes simplex virus and pseudorabies virus entry. *J Virol* **76**: 7203-7208.
39. Yu, Z, Chan, MK, O-charoenrat, P, Eisenberg, DP, Shah, JP and Singh, B *et al.* (2005). Enhanced nectin-1 expression and herpes oncolytic sensitivity in highly migratory and invasive carcinoma. *Clin Cancer Res* **11**: 4889-4897.
40. Krummenacher, C, Baribaud, F, Ponce de Leon, M, Baribaud, I, Whitbeck, JC and Xu, R *et al.* (2004). Comparative usage of herpesvirus entry mediator A and nectin-1 by laboratory strains and clinical isolates of herpes simplex virus. *Virology* **322**: 286-299.